

1. Introduction

Unmanned aircraft systems (UAS) hold significant potential to advance the understanding of tornadoes and, through targeted surveillance, directly improve the skill of storm-scale predictions and tornado forecasts. While the current regulatory environment over the United States places limits on the application of UAS towards these ends, demonstrated success targeting tornadic and non-tornadic supercells proves the general feasibility of this work. Moreover, using synthetic (simulated) data, advances can be made to determine optimal targeting of supercell thunderstorms by UAS without actual operations.

2. Prior Work

Second Verification of the Origins of Rotation in Tornadoes Experiment (VORTEX2)

- o Used the Tempest (Figure 1).
- o Six deployments on supercells (Table 1 and Figure 2)
- o Acquisition of 59 FAA Certificates of Authorization (Figure 2) with operation at 2 hours notice
- o Observations collected across the rear flank gust front (RFGF) and within the rear flank downdraft (RFD) outflow (Figure 3)
- o Sampled two rear flank internal surges (RFIS; Figure 3)



Figure 1. Tempest unmanned aircraft as configured for VORTEX2.

3. Ensemble Sensitivity Analysis

3.1. Methodology

Ensemble sensitivity analysis (ESA) is performed by perturbing the state of a model, integrating forward, and statistically relating the perturbations to the forecast response of the model (Ansell and Hakim 2007). Regions where there is a strong correlation between the perturbations and the response are assumed to be preferred locations for targeting observations.

Idealized WRF supercell simulations serve as the basis for the ESA conducted for this work.

1. A 101 member ensemble is created using perturbations to the base state sounding that are maximized below $z = 2 \text{ km}$: $\sigma = 0.5^\circ$ for T and T_d and $\sigma = 0.2 \text{ m s}^{-1}$ for u and v .
2. The ensemble is integrated forward 90 min.
3. Perturbations of temperature, water vapor mixing ratio, pressure, and all three components of the wind are logged.
4. The storm is integrated forward an additional 60 min.
5. Instead of evaluating the sensitivity using a single perturbation variable and single response variable, a multiple regression is calculated with all of the perturbations and each forecast response.

4. Future Work

4.1. Expanded ESA

Additional ESA work is required to establish the robustness of the current ESA results.

- o Need to quantify the sensitivity of current results to relative magnitudes of initial base state perturbations.
- o Additional environments and associated supercell morphologies and strengths need to be considered.
- o Storm interactions need to be considered.

4.2. Atmospheric Model for Online Planning

An atmospheric model for online planning (AMOP) is used to guide UAS path planning for collecting targeted observations. Two components:

1. Targeting heuristic developed offline with expanded storm-scale ESA
2. Target volume extrapolation method for advancing the volume diagnosed with the heuristic forward in time.

The AMOP will be used to test the assimilation of UAS observations of supercells into storm-scale numerical weather prediction models.

4.3. Observing System Simulation Experiments

An observing system simulation experiment (OSSE) is a model-based method of assessing the potential value of observing platforms on numerical weather prediction. Proposed OSSEs would aim to answer the following:

1. Can data collection within the target volumes predicted by the AMOP produce improved storm-scale predictions?
2. What sampling strategies within the target volumes maximize the impact on forecast skill?

5. Long-Range Vision

The current paradigm for surveilling the atmosphere cannot reliably collect the data that could significantly improve tornado warning accuracy. A system of targeted surveillance using UAS (Figure 5) would make these data available in near real-time to National Weather Service forecasters and to numerical weather prediction models that will eventually be used for storm-scale forecast guidance.

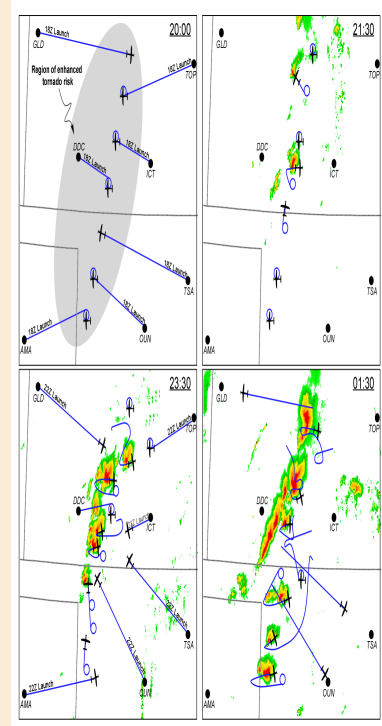


Figure 5. Hypothetical application of UAS in a mode of targeted surveillance for improving supercell and tornado forecasts.

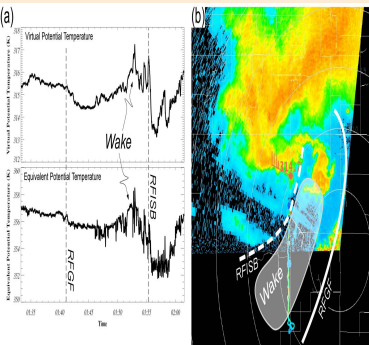


Figure 3. Examples of a rear flank gust front (RFGF) associated with the RFD and a rear flank internal surge (RFIS) and associated boundary (RFISB). a) Time series of virtual potential temperature and equivalent potential temperature from UAS transects executed on 10 June 2010 as part of VORTEX2 and b) radar reflectivity and boundary positions corresponding to the 10 June 2010 flight.

6. Summary

- o Demonstrated success deploying UAS on tornadic and non-tornadic supercells proves the general feasibility of targeted surveillance to advance understanding and improve the skill of storm-scale predictions and tornado forecasts.
- o Both the forward flank baroclinic zone and rear flank immediately west of the mesocyclone are regions with the largest impact on response variables
- o Wind observations appear to be more significant than temperature/moisture observations for impacting model sensitivity, but additional analysis is required to support this finding.

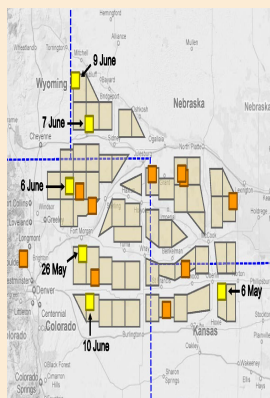


Figure 2. Regions covered by VORTEX2 certificates of authorization (beige polygons), VORTEX2 UAS deployments that were (were not) coordinated with the rest of the armada (yellow (orange) squares).

Table 1. Summary of VORTEX2 deployments.

Date	Armada Coordination	Flight Time (mm:ss)	Data Collection
05/06/2010	Yes	44:15	Inflow data only
05/26/2010	Yes	45:01	Inflow data only
06/06/2010	No	19:35	RFGF and RFD outflow
06/07/2010	No	27:30	RFD outflow
06/09/2010	Yes	33:30	RFGF, RFD outflow, and RFIS
06/10/2010	Yes	34:00	RFGF, RFD outflow, and RFIS

3.2. Results

- o Both the forward flank baroclinic zone and rear flank immediately west of the mesocyclone are regions with the largest impact on response variables (Figure 4).
- o Wind observations appear to be more significant than temperature/moisture observations for impacting model sensitivity (Table 2) but additional simulations and analysis are required to establish the robustness of this finding.

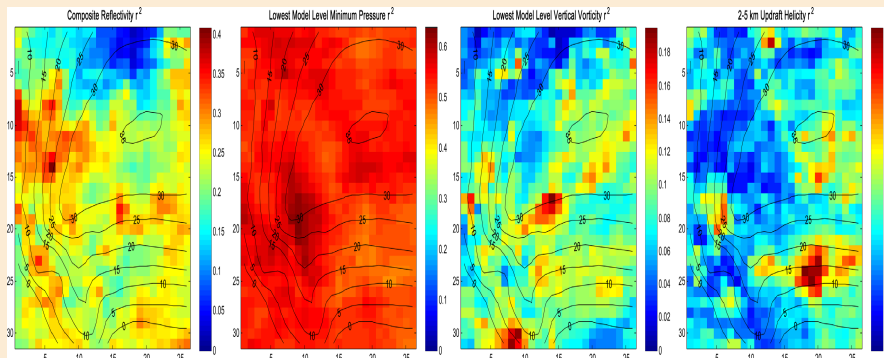


Figure 4. Distributions of correlation coefficient (colored shading) and ensemble mean reflectivity (black contours) for 4 of the response variables considered in the ESA.

Table 2. Difference in r^2 when either wind or temperature/dew point temperature are removed from the regression

	No wind	No T/d
2-5 km Updraft Helicity	-0.0971	-0.0418
Composite Reflectivity	-0.1238	-0.0146
Lowest Model Level T	-0.0393	-0.0199
Lowest Model Level Td	-0.1566	-0.0363
Lowest Model Level p	-0.0621	-0.0198
Lowest Model Level Wind Speed	-0.0537	-0.0072
Lowest Model Level Vertical Vorticity	-0.0724	-0.0385

Acknowledgements and Contact Information

This work has been funded by the National Science Foundation, the Air Force Office of Scientific Research, the Nebraska Research Council, the University of Colorado, and the Jonathan Merage Foundation.

Adam Houston: ahouston2@unl.edu
http://ussrg.unl.edu